

MOL#90431

Title Page

**Passenger protein determines translocation versus retention in the endoplasmic reticulum for
aromatase expression**

Jasmeet Kaur and Himangshu S. Bose

Mercer University School of Medicine and
Memorial University Medical Center, Department of Biochemistry,
Biomedical Sciences, Anderson Cancer Institute, Savannah, GA 31404

MOL#90431

Running Title: Signal sequence overrides signal anchor

Corresponding Author: Himangshu S. Bose, Department Biochemistry, Division of Biomedical Science, Mercer U School of Medicine and Memorial U Medical Center, Hoskins Research Building, 4700 Waters Avenue, Savannah, GA 31404, Tel: (912) 350-1710; Email: bosc_hs@mercer.edu and bosc_h1@memorialhealth.com

Number of text pages: 36

Number of Tables: 0

Number of figures: 7

Number of references: 54

Number of words in Abstract: 228

Number of words in Introduction: 720

Number of words in Discussion: 1,173

Supplemental material: 0

Abbreviations:

The abbreviations used are: Cell-Free transcription-translation (CFS), dihydrofolatereductase (DHFR), endoglycosidase H (endo H), endoplasmic reticulum (ER), methotrexate (MTX), microsomal membrane (MM), oligosaccharyltransferase (OST), preprolactin (pPL), proteinase K (PK), side-chain-cleavage enzyme (SCC), signal anchor type-I (SA-I), sodium dodecyl sulphate (SDS).

MOL#90431

ABSTRACT

Aromatase protein is over expressed in the women's breast affected with cancer. Because, in the endoplasmic reticulum (ER), signal sequence and signal anchors (SAs) facilitate translocation and topology of proteins. To understand the function of SA-Is, we evaluated translocation of aromatase, whose signal anchor follows a hydrophilic region. Aromatase SA-I mediates translocation of a short N-terminal hydrophilic domain to ER lumen and integrates the protein in the membrane, with the remainder of the protein residing in the cytosol. We showed that lack of a signal peptidase cleavage site is not responsible for the stop-transfer function of SA-I. However, SA-I could not block the translocation of a full-length microsomal secretory protein and was cleaved as part of the signal sequence. We propose that interaction between the translocon and the region following the signal anchor plays a critical role in directing the topology of the protein by SA-Is. The positive charges in the signal sequence helped it to override the function of signal anchor. Thus, when signal sequence follows SA-I immediately, the interaction with the translocon is perturbed and topology of the protein in ER is altered. If signal sequence is placed far enough from SA-I, then it does not affect membrane-integration of SA-I. In summary, we conclude that it is not just the SA-I, but also the region following it, which together affect function of aromatase SA-I in ER.

MOL#90431

INTRODUCTION

Protein translocation across eukaryotic membranes is the most critical step in biogenesis, as protein function depends on the correct subcellular localization. Co-translational translocation pathway plays a central role in the simultaneous synthesis and transport or integration of proteins into the endoplasmic reticulum (ER) membrane. While soluble and secretory proteins fully cross the ER membrane to reach the lumen, integral membrane proteins embed in the ER membrane through one or more of their transmembrane (TM) segments. Further, N-glycosylation and signal peptide cleavage are co-translational modifications of proteins in the ER, performed by oligosaccharyltransferase (OST) and signal peptidase complex (SPC), respectively (Hegde and Bernstein, 2006; Kelleher and Gilmore, 2006). However, all the proteins use the same machinery i.e. a protein conducting channel formed by Sec61 complex called translocon, for their transport across the membrane. The co-translational translocation pathway requires the protein to have a signal sequence at the N-terminus. Signal sequences of secretory proteins and type I membrane proteins, characterized by a stretch of 7-25 mainly apolar amino acid residues, are proteolytically removed during or at the end of protein transport (Walter and Johnson, 1994). Signal sequences directly target the nascent polypeptides to sites of translocation at the ER membrane and dictate the topology of the protein (Egea et al., 2005; Keenan et al., 2001; Walter and Johnson, 1994). The presence of a stop-transfer sequence blocks further translocation of membrane proteins, facilitating their insertion into the lipid bilayer. The N-terminal hydrophobic segments of microsomal cytochrome P450s work as a type-I signal anchor (SA-I) (Nelson and Strobel, 1988), and have the combined topogenic functions of a signal sequence and a stop-transfer sequence (Monier et al., 1988; Sakaguchi et al., 1987a; Szczesna-Skorupa et al., 1988). SA-Is generate integral membrane proteins with a $N_{\text{exo}}/C_{\text{cyt}}$ orientation in the ER membrane (Monier et al.,

MOL#90431

1988). Aromatase is a glycosylated microsomal cytochrome P450 protein (Shimozawa et al., 1993). Aromatase protein has a SA-I, however, a short hydrophilic domain precedes aromatase's signal anchor, making it an atypical member of the P450 family (Chen and Zhou, 1992). Aromatase catalyzes the formation of estrogens. Breast tumors express greater levels of aromatase (Killinger et al., 1987; Miller and O'Neill, 1987; Reed et al., 1989; Silva et al., 1989), leading to a many-fold increase in intratumoral estradiol as compared with plasma and subsequent disease development (Thijssen and Blankenstein, 1989) (Figure 1A). As a result, aromatase has become an attractive breast cancer therapeutic target, underscoring the need to better understand how the cell regulates its activity.

The topology of proteins co-translationally integrated into the ER stems from topogenic sequences in their primary structures (Blobel, 1980; Sabatini et al., 1982). The distribution of charged amino acids on either end of the signal sequence and the hydrophobicity of the apolar core of the signal sequence or signal anchor determine signal orientation (Sakaguchi et al., 1992b). The more positively charged flanking sequence is on the cytosolic side of the membrane due to the electrostatic interactions at or near the translocon (von Heijne, 1986). Accordingly, mutations of charged residues flanking a signal sequence can affect its orientation significantly (Andrews et al., 1992; Beltzer et al., 1991; Parks and Lamb, 1991; Parks and Lamb, 1993). Moreover, the tendency for translocation of the N-terminus into the ER lumen increases with an increase in hydrophobicity of the N-terminal region (Eusebio et al., 1998; Harley et al., 1998; Roésch et al., 2000; Sakaguchi et al., 1992b; Wahlberg and Spiess, 1997). Signal sequences and signal anchors are inter-convertible by mutations that lead to changes in charge and hydrophobicity of these regions (Kuroiwa et al., 1991; Szczesna-Skorupa et al., 1988). Thus, the exact mechanism by which newly synthesized proteins translocate across the ER membrane

MOL#90431

remains unclear. It is still unknown why some proteins completely translocate across the ER bilayer while others stay partially embedded. While the possibility exists that the nature of the protein chain being translocated affects the signal sequence/anchor function and that the position of these sequences affect their function, this has not been fully explored. Also, questions remain as to what the molecular basis is for the stop-transfer function of signal anchors.

In this study, we show that the SA-I cannot block the translocation of a passenger secretory protein. As well, we show for the first time that a passenger signal sequence could block the function of an upstream signal anchor.

MOL#90431

MATERIALS AND METHODS

Reagents. All reagents, unless specified otherwise, were purchased from Sigma-Aldrich (St. Louis, MO).

Construction of cDNAs. Full length cDNA encoding human aromatase and other cDNAs were subcloned into the SP6 vector, downstream of the SP6 RNA polymerase promoter. Site-directed mutagenesis was performed by PCR amplification using Pfu-DNA polymerase. Cycles consisted of denaturation at 94° C denaturation, annealing at 55° C annealing and extension at 72° C extension, with a final extension for 5 min at 72° C. The PCR-amplified product was purified using gel electrophoresis and a QIAquick Gel extraction kit (Qiagen, Germany). The purified amplified product was digested with BglII/EcoR1 restriction enzyme (New England Biolabs, MA) and ligated to predigested SP6 vector with T4 DNA ligase (New England Biolabs, MA). The ligation was then transformed to DH5 α competent cells and the plasmid was purified through QIAprep Spin Miniprep kit (Qiagen, Germany). The accuracy of the plasmids was checked by dideoxy chain termination method in both the strands from a commercial source (MC Lab, CA).

Cell-free transcription-translation and synthesis of chimeric proteins. A cell-free transcription/translation synthesis (CFS) was performed to express proteins for *in vitro* experiments using wheat germ extract (Promega, Madison, WI) labeled with [³⁵S]methionine (MP Biomedicals, Solon, OH). The wheat extract provides ribosomes and cofactors for protein expression. The cDNAs of interest coupled to an SP6 promoter were added, along with SP6 polymerase (Promega, WI), in the presence and absence of rough microsomal membranes (MM) from dog pancreas. Rough microsomal membranes and signal recognition particle (SRP) (tRNA probes, College Station, TX), when indicated, 1 μ l was added per 12.5 μ l of translational reaction. The mixture was incubated at 22° C for 2 h, separated by SDS-polyacrylamide gel

MOL#90431

electrophoresis and visualized through phosphorimager or by autoradiography. The figures were prepared from the same experiment or two identical experiments performed at two different times without changing the integrity of the figure.

Glycosylation, proteolysis and membrane integration assay. Aliquots of the translation product were incubated at 100° C for 10 min with 10X glycoprotein denaturing buffer and then the denatured samples were treated with Endo H (New England Biolabs Inc, MA) at 37° C for 1 h following manufacturer's protocol (The reagents and buffers were supplied by the manufacturer). For proteolysis, aliquots of translated product were treated with 1 µg/ml of proteinase K (PK) at RT for 15 min. Proteolysis was terminated by the addition of PMSF to a final concentration of 2 mM and 2X SDS sample buffer, and the mixture was transferred to a boiling water bath. For membrane integration study, microsomes were collected with ultracentrifugation at 109,000 x g (Beckman TL-100.2) at 4° C for 30 min. The supernatant was collected and the pellet was treated with freshly prepared 100 mM sodium carbonate solution (pH 11.4) on ice for 15 min. The samples were ultracentrifuged to separate soluble fraction (S) from the membraneous fraction (P). In experiment with methotrexate (MTX), 100 nM was used as the final concentration. All radioactive electrophoresed bands were visualized through phosphorimager and by autoradiography.

MOL#90431

RESULTS

Aromatase is an integral membrane protein with a N_{exo}/C_{cyt} topology.

Microsomal P450s reside in the cytosol but are integrated into the ER membrane by their membrane anchors. N-glycosylation occurs in the ER lumen and so while P450 proteins have putative N-glycosylation sites, they typically remain unglycosylated. However, the N-terminal of the P450 protein aromatase is atypical as compared with other microsomal P450s, in that its signal anchor region follows a hydrophilic domain. Glycosylation of aromatase, which has putative sites at Asn-12 and Asn-180, in the presence of microsomal membranes (MM) (Shimozawa et al., 1993) signify that, unlike other P450 proteins, these sites are accessible to oligosaccharyltransferase (OST). OST, located within the ER lumen, adds oligosaccharides to Asn-X-Ser/Thr acceptor tripeptides (Dalbey et al., 1997). Cell-free translation of aromatase in the absence of MM showed a protein band (Figure 1B). When rough microsomes were added to the translation mixture, we observed an additional protein with a decreased mobility (Figure 1B), indicating that targeting aromatase to the ER results in its modification. We next treated the translated product with endoglycosidase H (endo H) (Figure 1B). Endo H is a highly specific endoglycosidase that cleaves asparagine-linked mannose rich oligosaccharides (Sakaguchi et al., 1992a). As expected endo H completely digested the higher molecular weight band (Figure 1B), confirming the glycosylation of aromatase. We treated an aliquot of the cell-free translated aromatase with proteinase K (PK) in presence and absence of detergent (Triton X-100) (Figure 1C). PK completely digested both the glycosylated and non-glycosylated protein (Figure 1C), suggesting that the ER membrane did not protect aromatase. Addition of detergent during proteolysis had a protective effect on aromatase as PK-mediated digestion was significantly reduced in the presence of Triton-X100 (Figure 1C). The result suggests that detergent may act

MOL#90431

as a chaperone (Hegde et al., 1998) forming a structure that prevents PK from completely proteolyzing aromatase.

To examine the extent of integration of aromatase into the ER membrane, aliquots of translated product, with and without MM, were incubated with freshly prepared Na_2CO_3 , and then ultracentrifuged to separate the membrane pellet from supernatant fractions (Figure 1D). Na_2CO_3 breaks protein-protein interactions (Li and Shore, 1992) but not lipid-protein interactions, so all the peripheral membrane and soluble luminal proteins are recovered in the soluble fractions and membrane integrated proteins in the pelleted membrane (Chuck and Lingappa, 1992). In the absence of MM, washing with buffer as a control and alkali treatment resulted in recovery of the protein predominately in the soluble fraction (Figure 1D). Addition of MM led to the recovery of glycosylated aromatase in the pellet fraction, both in buffer and alkali-treated samples, suggesting that the protein needed a membrane environment for integration (Figure 1D, right-hand side).

To confirm the specificity of Asn glycosylation, we generated multiple aromatase N-terminal deletion mutants. The deletion constructs N Δ 50, N Δ 40, N Δ 30 and N Δ 20 did not appear glycosylated (Figure 1E). However, we observed glycosylation, albeit at lower levels, of N Δ 10 (Figure 1E). These results suggest that Asn-12 was the only site glycosylated in aromatase. To confirm that only Asn-12 is glycosylated, we generated the internal deletion mutants N Δ 11-40, N Δ 11-30 and N Δ 11-20, and found that these lacked glycosylation when translated in the presence of MM (Figure 1F). We further narrowed the region to N Δ 12-14, N Δ 12-15 and N Δ 12-16, and again saw no glycosylation (Figure 1G). To confirm further on the specificity of amino acids, we made point mutations by substituting a polar to a nonpolar residue and from a bulky to a small or neutral amino acid. First, we mutated 12th amino acid, asparagine to threonine and

MOL#90431

second, we mutated 14th amino acid, threonine to alanine. Identical cell-free transcription translation experiments in presence of microsomal membrane showed no glycosylation (Figure 1H). Therefore, of the two potential glycosylation sites, Asn-12 and Asn-180, only Asn-12 was glycosylated and hence localized to the lumen.

Furthermore, glycosylation of aromatase in the absence of first 10 amino acids from the N-terminus shows that translocation of aromatase into the ER did not require the N-terminal hydrophilic sequence. However, the observed weaker glycosylation suggests that its absence possibly interfered with the accessibility of OST to the glycosylation site. Thus, the observed glycosylation of aromatase in the presence of MM, complete accessibility to PK and resistance to alkali treatment indicate that aromatase is an integral membrane protein with N_{exo}/C_{cyt} topology in the ER (Figure 1I).

Aromatase N-terminus 40 residues controls translocation of passenger proteins.

We further addressed the role of the aromatase N-terminus on mediating translocation by replacing the signal sequence of preprolactin (pPL), a secretory protein with a cleavable 30 residue signal sequence (Stern and Jackson, 1985), with increasing lengths of the aromatase N-terminus (first 12, 20, 30, 40 and 50 residues) (Figure 2A). A hydrophobic amino terminus is indicative of a membrane anchor in microsomal cyp450s (Chen and Zhou, 1992). However, in aromatase, a more hydrophilic domain of about 20 residues precedes the hydrophobic region (Chen and Zhou, 1992). Thus we wanted to confirm that it is actually the hydrophobic region following the short N-terminal hydrophilic domain which is working as SA-I. We left the four amino acids preceding the cleavage site in pPL intact (Figure 2A). In the presence of microsomal membrane, pPL undergoes processing to form the lower molecular weight protein, PL, which is resistant to protease digestion in the absence of detergent (Nicchitta and Blobel, 1989). However,

MOL#90431

we found that none of the aromatase-pPL fusion proteins underwent processing to a lower molecular weight protein (Figure 2B). This result (Figure 2B) confirms that the aromatase N-terminus works as a signal anchor, thereby blocking the ability of the pPL signal peptidase cleavage site to reach the lumen and undergo processing.

Furthermore, we observed that the fusion proteins containing the first 12, 20 and 30 amino acids of aromatase were not glycosylated (Figure 2B), whereas the fusion protein containing the first 40 aromatase amino acids was glycosylated (Figures 2B and C). Thus, we conclude that the first 40, but not 30, amino acids of aromatase can act as a signal anchor, placing the N-terminal domain in ER lumen and halting the translocation of the passenger protein pPL. Aromatase N-terminus from residues 20-40 is the hydrophobic region (Chen and Zhou, 1992) and thus working as SA-I. Moreover, the crucial region of the aromatase signal anchor appears to be located between 31-40 amino acid residues.

To confirm our above finding, we similarly fused the N-terminal 40 residues of aromatase with the cytosolic protein dihydrofolatereductase (DHFR) (Figure 3A, Top panel). DHFR is a 25 kDa cytosolic protein with 187 residues that has been widely used as a passenger protein to various organelles (Hurt et al., 1985). Translation of the fusion protein [1-40Ar+1-187DHFR] in the presence of MM resulted in its glycosylation, while incubation with endo H resulted in deglycosylation (Figure 3A, Bottom panel). To confirm our results, we translated the fusion protein in the presence and absence of methotrexate (MTX), a specific ligand of DHFR (Blakley and Cocco, 1985) (Figure 3B). MTX treatment did not affect glycosylation of the fusion protein (Figure 3B). We next fused first 40 residues of aromatase with a full-length mitochondrial-targeting cytochrome P450 protein, side-chain-cleavage enzyme (SCC), generating 1-40Ar+1-521SCC (Figure 3C, Top panel). SCC's first 39 residues work as a cleavable N-terminal

MOL#90431

sequence that mediates translocation into the mitochondria (Chung et al., 1986). However, translation in the presence of MM resulted in a glycosylated fusion protein, sensitive to endo H and resistant to cleavage to a lower molecular weight protein (Figure 3C, Bottom panel). Thus, the results confirm that the aromatase N-terminus 40 residues work as the signal anchor.

The concluding region of aromatase SA-I sequence is indispensable for its function.

We have now established that the first 40 residues of aromatase can target passenger proteins to the ER; however, the crucial part of the signal anchor lies between residues 31-40, as first 30 residues could not mediate glycosylation. Sequence analysis of aromatase from various species (Chen and Zhou, 1992) and the three-dimensional crystal structure of aromatase purified from human placenta (Ghosh et al., 2009) suggest that residues 21-42 integrate into lipid, forming a transmembrane segment. Based on the evidence, we hypothesized that residues 21-42 of aromatase serve as the signal anchor region and prepared a series of internal deletion mutants to test this. In the first set of mutants, we kept the N-terminal hydrophilic domain spanning residues 1 to 20 and the glycosylation site (Asn-12), intact (Figure 4A, Top panel). When translated in the presence of MM, N Δ 21-50 and N Δ 21-40 (Figure 4A, Bottom panel) were not glycosylated, indicating that the region is crucial for translocation and thus glycosylation of aromatase. To determine the specificity of this region, we divided residues 21-40 into two equal parts, generating the mutants N Δ 21-30 and N Δ 31-40 (Figures 4A and B, Top panels). When these mutants were translated with MM, we observed glycosylation of the N Δ 21-30 protein (Figure 4A, Bottom panel), but not of the N Δ 31-40 protein (Figures 4B, Bottom panels). Deletion mutants' result confirmed that residues 31 to 40 are necessary to place aromatase N-terminus in ER lumen. Mutant proteins, N Δ 41-60 and N Δ 51-60 further supported our conclusion as both these mutant proteins were glycosylated in the presence of MM (Figure 4C, Bottom panel),

MOL#90431

suggesting that residues 41 and higher did not contribute to the glycosylation of aromatase. We next generated additional mutants NΔ26-35, NΔ36-45 and NΔ46-55 (Figure 4D, Top panel). Assays revealed the glycosylation of both NΔ26-35 and NΔ46-55, but not of NΔ36-45 (Figure 4D, Bottom panel) indicating that residues from the 36th position in the signal anchor region are most crucial for aromatase SA-I function. The hydrophobic regions of the cytochrome P450 signal anchors are about 20 amino acid residues in length, much shorter than other type I signal anchor proteins, such as mouse synaptotagmin II (Kida et al., 2000). Nevertheless, deleting a major part of the signal anchor region had no effect on the glycosylation of aromatase. From above results, we infer that the last five residues of aromatase signal anchor (36-40) are critical for its function. This was indeed the case, as NΔ36-40 mutant protein was not glycosylated in the presence of MM (Figure 5A, Bottom panel). However, it is possible that deletion of these last five amino acids affect positioning enough to inhibit glycosylation, even if the insertion and topology are in correct orientation. To confirm this, we did sodium carbonate extraction of NΔ36-40 mutant protein in presence and absence of MM (Figure 5B). The mutant protein was recovered in the soluble fraction (Figure 5B). The result corroborated our inference that residues 36 to 40 are indispensable for membrane integration and thus glycosylation of aromatase, even if rest of the signal anchor remains intact. We next prepared mutant proteins with point substitutions to investigate the individual residues in region N36-40. The region (36-40 residues) consists of the hydrophobic amino acids LLVWN, which we sequentially replaced with the hydrophobic residues VVLFQ (Figure 5C, Top panel). All the mutants were found to be glycosylated in the presence of MM (Figure 5C). It appears that the hydrophobicity of this short region may support the correct orientation of aromatase in the ER membrane. So, absence of the last five residues of SA-I (N36-40) blocks aromatase glycosylation, even when rest of the SA-I

MOL#90431

remained intact, making it the most critical region of SA-I. To determine whether residues 36-40 are crucial for interaction with SRP also, we translated NΔ36-40 in cell-free system in presence and absence of SRP (Figure 5D, Left panel). SRP arrests the translation of protein with membrane-insertion signals in cell-free system (Holland and Drickamer, 1986; Spiess and Lodish, 1986). We saw that the translation of NΔ36-40 protein was arrested by the addition of SRP (Figure 5D), confirming that SRP does not need residues 36-40 for its interaction with signal anchor of aromatase. Addition of SRP to the translation system did not affect the translation of globin (Figure 5D), as globin is a cytosolic protein with no signal peptide sequence. Translation of full-length aromatase was also reduced in presence of SRP (Figure 5D) confirming that signal anchor of aromatase interacts with SRP. In summary our current results show that aromatase translocates in ER by using its signal anchor to open the lateral gate of translocon to get membrane integrated (Figure 5E).

Passenger signal sequence overrides upstream-placed signal anchor.

The underlying mechanism of signal anchor function remains unclear. While SA-I functions as a classical signal sequence and as a stop-transfer sequence (Monier et al., 1988; Sakaguchi et al., 1987b; Szczesna-Skorupa et al., 1988), the lack of a signal peptidase cleavage site is not responsible for the stop-transfer function of signal anchors. To better understand the function of SA-Is, we investigated whether it could convert the topology of a full-length secretory protein, such as pPL, by blocking the translocation of its signal sequence. We fused 40 and 50 residues of the N-terminal of aromatase in front of full-length pPL (Figure 6A, Top panel), generating 1-40 and 1-50Ar+1-229pPL. When these fusion proteins were translated in the cell free system with MM, we observed the appearance of lower molecular weight proteins (Figures 6C and D). Processing to a lower molecular weight protein can only happen if proteins translocate across the

MOL#90431

ER membrane and reach the lumen, where signal peptidase cleave the signal sequence to generate lower molecular weight proteins. As aromatase signal anchor lacks a signal peptidase cleavage site, the observed lower molecular weight proteins, resulted likely from processing at the cleavage site in pPL. The identical molecular weight of the processed fusion proteins supports this possibility and suggests that the N-terminus of aromatase, which is a signal anchor, could not block the translocation of the passenger full-length pPL. Instead, the signal anchor of aromatase was cleaved as part of the signal sequence in these fusion proteins, indicating that the pPL signal sequence overrode the function of the aromatase signal anchor. Thus, the signal sequence converted the SA-I to a signal sequence, resulting in a soluble protein.

To determine the general applicability of our findings, we next generated a fusion protein consisting of membrane-anchor signal peptide of Cytochrome P450IIC2 (Szczesna-Skorupa et al., 1988), followed by full-length pPL (1-26 CYPIIC2+1-229 pPL; Fig. 6A, Bottom panel). CYPIIC2 also has a type-I signal anchor and integrates into the membrane with a $N_{\text{exo}}/C_{\text{cyt}}$ topology (Szczesna-Skorupa et al., 1988). When the negative charge in the signal anchor of CYPIIC2 was replaced with positive charges, the mutant protein behaved similar to a secretory protein (Szczesna-Skorupa et al., 1988). Translation of the CYPIIC2-pPL fusion protein in the presence of MM also resulted in the appearance of a protein with a lower molecular weight (Figure 6E). Thus, CYPIIC2 signal anchor also could not block the translocation of the downstream pPL signal sequence, resulting in its cleavage. The results (Figures 6C and E) confirm that a secretory signal sequence can override type-I signal anchors when placed downstream to the latter and thus, type-I signal anchors cannot block translocation of secretory signal sequences. To confirm that the lower molecular weight protein is a secretory protein, we treated the newly synthesized fusion protein (1-40Ar+1-229pPL) with sodium carbonate (Figure

MOL#90431

6F). In the presence of MM, the lower molecular weight protein was completely recovered in the soluble fraction, confirming our results.

Signal sequence is characterized by being more positively charged compared to signal anchor and mutations in charges interconvert signal sequence and signal anchor (Kuroiwa et al., 1991; Szczesna-Skorupa et al., 1988). To get a deeper insight into our above observation, we mutated the positive charges in the signal sequence of pPL in the fusion protein 1-40Ar+1-229pPL. The amino acid changes are presented schematically (Figure 7A). The mutated proteins were then translated in presence and absence of MM (Figure 7B). We observed that the processing of these mutated proteins were very similar, except the mutant protein, KKR to DDD (Figure 7B). The processing of the KKR to DDD mutant protein into the ER as a soluble protein was significantly inhibited, confirming that positive charges of signal sequence played a major role for overriding the signal-anchor function (Figure 7C).

To understand the mechanistic detail of signal anchor, we performed a competition experiment between the signal sequence and signal anchor. We placed signal sequence of pPL at distance of 10 and 160 amino acids from the signal anchor, generating 1-50Ar+1-229pPL and 1-200Ar+1-229pPL (Figure 7D, Top panel). We next studied the translocation of the fusion proteins after translation in presence and absence of MM (Figure 7D, Bottom panel). The results show that the fusion protein 1-50Ar+1-229pPL was processed to a lower molecular weight protein (Figure 7D, bottom panel). However, fusion protein 1-200Ar+1-229pPL (Figure 7D, Bottom panel) showed re-appearance of glycosylation. Glycosylation of 1-200Ar+1-229pPL fusion protein can happen if the signal anchor of aromatase is integrated into the membrane. Membrane-integration of signal anchor in fusion protein 1-200Ar+1-229pPL is possibly because the signal sequence was far apart to interfere with the interaction between signal anchor and the

MOL#90431

translocon. Therefore, by delaying the translation of signal sequence, signal anchor got enough time to perform its function as stop-transfer (Figure 7E).

MOL#90431

DISCUSSION

We embarked on this study to better understand the mechanism of signal anchor-mediated targeting of newly synthesized proteins to the ER. Unlike signal sequences, SA-Is work as both membrane-integration and stop-transfer signals (Monier et al., 1988; Sakaguchi et al., 1987b). In addition, a recent report describes the ability of SA-I to mediate the translocation of a preceding amino-terminal domain (Kida et al., 2005). While many families of proteins have topogenic SA-I regions, it most commonly occurs in the microsomal cytochrome P450 family (Kida et al., 1998).

The specificity of signal sequence and anchor activity depends on the balance between the hydrophobic segment and the N-terminal charges (Sakaguchi et al., 1992b). Signal anchors are uncleavable signal sequences. While the absence of a signal peptidase cleavage site is important (Holland and Drickamer, 1986; Zerial et al., 1986), studies have shown that the length and hydrophobicity of the hydrophobic core (Spiess and Lodish, 1986) as well as the lack of positive charge (Szczesna-Skorupa et al., 1988) also may also contribute to the lack of cleavage of SA-I. Not surprisingly, modifications that alter the balance between hydrophobicity and charge can convert signal anchors to cleaved signal sequences, if provided with a cleavage site (Kuroiwa et al., 1991; Szczesna-Skorupa et al., 1988). In our study, we showed that the SA-I mediated the translocation of the preceding hydrophilic domain into the ER lumen, leading to its glycosylation. Furthermore, we found that part of the protein integrated into the ER membrane while the rest resided in the cytosol. In the absence of the signal anchor, the hydrophilic domain did not translocate the ER membrane. We also concluded that the first 40 residues of aromatase were sufficient to work as a signal anchor, based on the ability of this peptide to target cytosolic and mitochondrial passenger proteins to the ER. However, the signal anchor of aromatase could not block the translocation of a immediately following full-length secretory protein. In this case,

MOL#90431

the signal anchor was cleaved as part of the signal sequence and the signal anchor no longer functioned as a stop-transfer sequence, which resulted in the generation of a soluble secretory protein. This outcome suggests that the signal sequence of the passenger secretory protein altered the topological function of the signal anchor.

The possibility exists that the complete change in the signal anchor function that we observed in the fusion protein may have resulted from altered interaction with the translocon. The translocon mediates translocation across and integration of proteins into the endoplasmic reticulum membrane (Johnson and van Waes, 1999; Osborne et al., 2005). The translocon consists of Sec61 complex with 10 transmembrane domains that form a hydrophilic channel with a lateral exit site. The central hydrophilic pore is blocked by a central constriction and a plug domain on the luminal side. The plug on the luminal side needs to open and the ring must enlarge to allow protein translocation (Saparov et al., 2007; Tam et al., 2005). Furthermore, the translocon has been shown to open laterally towards the lipid bilayer and the degree of opening is likely to vary according to the hydrophobic property of the signal and signal anchor sequence (Martoglio et al., 1995). Because, a direct interaction between membrane integrating sequences (transmembrane segments) and the lipid phase responsible for recognition of these regions at the translocon (Hessa et al., 2005). The loss of SA-I function that we observed it was followed a signal sequence immediately, may have resulted from the destabilization of the closed state of translocon pore (Figure 7C). Destabilization could lead to a premature opening of the pore towards the ER lumen (Junne et al., 2007), allowing translocation to occur rather than the transfer of the signal anchor to the lipid bilayer. Secretory signal sequences are characterized by positive charges and signal anchors by negative charges. Mutations leading to a net positive charge in a signal anchor can subsequently convert it to a signal sequence (Kuroiwa et al., 1991;

MOL#90431

Szczesna-Skorupa et al., 1988). Thus, our results strongly suggest that negatively charged signal anchors interact with translocon to keep its luminal exit in a closed position (Figures 5E and 7E). The signal anchor then interacts with the lateral exit site, resulting in transfer to the lipid phase. This association of SA-I with the translocon may explain why the addition of a cleavage site after the aromatase signal anchor did not result in translocation of the protein to the lumen where it can be cleaved. However, when the positive charge of a signal sequence follows the signal anchor, the possibility exists that the luminal end plug opens, to reduce repulsion of the more positively charged end of the signal sequence (Figure 7C) and thus mediating translocation in the ER lumen. Significantly reduced processing to soluble protein in the mutant protein (KKR to DDD) supports our hypothesis.

Our results also suggest that time may elapse before the membrane anchor is transferred from the proteinaceous channel to the lipid phase, and thus the signal sequence was able to override the effect of the flanking domains, leading to their translocation in the ER lumen. Had the membrane integration occurred before the signal sequence opened the luminal exit of the translocon, the protein would have not been able to translocate (Figure 7E). Thus our results show that insertion of the membrane anchor into the lipid bilayer play a very critical role in the stop-transfer function of signal anchors. Further, it is not only the charges or the hydrophobicity of sequences that decide the topology of proteins in the ER, but also the amino acid sequences following them. To our knowledge, this is the first report showing that the passenger signal sequences could override a signal anchor, thereby regulating the topology of the protein.

MOL#90431

ACKNOWLEDGEMENTS

We are thankful to Drs. Evan Simpson (Prince Henry's Institute) for human aromatase cDNA, Vishwanath Lingappa (Prosetta Antiviral, Inc) and Arthur Johnson (Texas A&M, TX) for generously providing preprolactin and globin cDNAs.

AUTHORSHIP CONTRIBUTIONS

Participated in research design: Kaur and Bose

Conducted experiments: Kaur

Performed data analysis: Kaur and Bose

Wrote or contributed to the writing of the manuscript: Kaur and Bose

MOL#90431

REFERENCES

Andrews DW, Young JC, Mirels LF and Czarnota GJ (1992) The role of the N-region in signal sequence and signal-anchor function. *J Biol Chem* **267**: 7761-7769.

Beltzer JP, Fiedler K, Fuhrer C, Geffen I, Handschin C, Wessels HP and Spiess M (1991) Charged residues are major determinants of the transmembrane orientation of a signal-anchor sequence. *J Biol Chem* **266**: 973-978.

Blakley RL and Cocco L (1985) Binding of methotrexate to dihydrofolate reductase and its relation to protonation of the ligand. *Biochemistry* **24**: 4704-4709.

Blobel G (1980) Intracellular protein topogenesis. *Proc Natl Acad Sci USA* **77**: 1496-1500.

Chen S and Zhou D (1992) Functional domains of aromatase cytochrome P450 inferred from comparative analysis of amino acid sequences and substantiated by site-directed mutagenesis experiments. *J Biol Chem* **267**: 22587-22594.

Chuck SL and Lingappa VR (1992) Pause transfer -A topogenic sequence in apolipoprotein-B mediates stopping and restarting of translocation. *Cell* **68**: 9-21.

Chung B, Matteson KJ, Voutilainen R, Mohandas TK and Miller WL (1986) Human cholesterol side-chain cleavage enzyme, P450scc: cDNA cloning, assignment of the gene to chromosome 15, and expression in the placenta. *Proc Natl Acad Sci USA* **83**: 8962-8966.

MOL#90431

Dalbey RE, Lively MO, Bron S and van Dijl JM (1997) The chemistry and enzymology of the type I signal peptidases. *Protein Sci* **6**: 1129-1138.

Egea PF, Stroud RM and Walter P (2005) Targeting proteins to membranes: structure of the signal recognition particle. *Curr Opin Struct Biol* **15**: 213-220.

Eusebio A, Friedberg T and Spiess M (1998) The role of the hydrophobic domain in orienting natural signal sequences within the ER membrane. *Exp Cell Res* **241**: 181-185.

Ghosh D, Griswold J, Erman M and Pangborn W (2009) Structural basis for androgen specificity and oestrogen synthesis in human aromatase *Nature* **457**: 219-223.

Harley C, Holt JA, Turner R and Tipper DJ (1998) Transmembrane protein insertion orientation in yeast depends on the charge difference across transmembrane segments, their total hydrophobicity and its distribution. *J Biol Chem* **273**: 24963-24971.

Hegde RS and Bernstein HD (2006) The surprising complexity of signal sequences. *Trends Biochem* **31**: 563-571.

Hegde RS, Mastrianni JA, Scott MR, DeFea KA, Tremblay P, Torchia M, DeArmond SJ, Prusiner SB and Lingappa VR (1998) A transmembrane form of the prion protein in neurodegenerative disease. *Science* **279**: 827-834.

MOL#90431

Hessa T, Kim H, Bihlmaier K, Lundin C, Boekel J, Andersson H, Nilsson I, White SH and von Heijne G (2005) Recognition of transmembrane helices by the endoplasmic reticulum translocon. *Nature* **433**: 377-381.

Holland EC and Drickamer K (1986) Signal recognition particle mediates the insertion of a transmembrane protein which has a cytoplasmic NH₂ terminus. *J Biol Chem* **261**: 1286-1292.

Hurt EC, Pesold-Hurt B, Suda K, Oppliger W and Schatz G (1985) The first twelve amino acids (less than half of the pre-sequence) of an imported mitochondrial protein can direct mouse cytosolic dihydrofolate reductase into the yeast mitochondrial matrix. *EMBO J* **4**: 2061-2068.

Johnson AE and van Waes MA (1999) The translocon: a dynamic gateway at the ER membrane. *Annu Rev Cell Dev Biol* **15**: 799-842.

Junne T, Schwede T, Goder V and Spiess M (2007) Mutations in the Sec61p channel affecting signal sequence recognition and membrane protein topology. *J Biol Chem* **282**: 33201-33209.

Keenan RJ, Freymann DM, Stroud RM and Walter P (2001) The signal recognition particle. *Annu Rev Biochem* **70**: 755-775.

Kelleher DJ and Gilmore R (2006) An evolving view of the eukaryotic oligosaccharyltransferase. *Glycobiology* **16**: 47-62.

MOL#90431

Kida Y, Mihara K and Sakaguchi M (2005) Translocation of a long amino-terminal domain through ER membrane by following signal-anchor sequence. *EMBO J* **24**: 3202-3213.

Kida Y, Ohgiya S, Mihara K and Sakaguchi M (1998) Membrane topology of NADPH-cytochrome P450 reductase on the endoplasmic reticulum. *Arch Biochem Biophys* **351**: 175-179.

Kida Y, Sakaguchi M, Fukuda M, Mikoshiba K and Mihara K (2000) Membrane topogenesis of a type I signal-anchor protein, mouse synaptotagmin II, on the endoplasmic reticulum. *J Cell Biol* **150**: 719-730.

Killinger DW, Perel E, Daniilescu D, Kharlip L and Blackstein ME (1987) Aromatase activity in the breast and other peripheral tissues and its therapeutic regulation. *Steroids* **50**: 523-536.

Kuroiwa T, Sakaguchi M, Mihara K and Omura T (1991) Systematic analysis of stop-transfer sequence for microsomal membrane. *J Biol Chem* **266**: 9251-9255.

Li JM and Shore GC (1992) Reversal of the orientation of an integral protein of the mitochondrial outer membrane. *Science* **256**: 1815-1817.

Martoglio B, Hofmann MW, Brunner J and Dobberstein B (1995) The protein-conducting channel in the membrane of the endoplasmic reticulum is open laterally toward the lipid bilayer. *Cell* **81**: 207-214.

MOL#90431

Miller WR and O'Neill J (1987) The importance of local synthesis of estrogen within the breast. *Steroids* **50**: 537-548.

Monier S, Luc PV, Kreibich G, Sabatini DD and Adesnik M (1988) Signals for the incorporation and orientation of cytochrome P450 in the endoplasmic reticulum membrane. *J Cell Biol* **107**: 457-470.

Nelson DR and Strobel HW (1988) On the membrane topology of vertebrate cytochrome P-450 proteins. *J Biol Chem* **263**: 6038-6050.

Nicchitta CV and Blobel G (1989) Nascent secretory chain binding and translocation are distinct processes: differentiation by chemical alkylation. *J Cell Biol* **108**: 789-795.

Osborne AR, Rapoport TA and van den Berg B (2005) Protein translocation by the Sec61/SecY channel. *Annu Rev Cell Dev Biol* **21**: 529-550.

Parks GD and Lamb RA (1991) Topology of eukaryotic type-II membrane proteins - importance of N-terminal positively charged residues flanking the hydrophobic domain. *Cell* **64**: 777-787.

Parks GD and Lamb RA (1993) Role of NH₂-terminal positively charged residues in establishing membrane protein topology. *J Biol Chem* **268**: 19101-19109.

MOL#90431

Reed MJ, Owen AM, Lai LC, Coldham NG, Ghilchik MW, Shaikh NA and James VH (1989) In situ oestrone synthesis in normal breast and breast tumour tissues: effect of treatment with 4-hydroxyandrostenedione. *Int J Cancer* **1989**: 233-237.

Roésch K, Naeher D, Laird V, Goder V and Spiess M (2000) The topogenic contribution of uncharged amino acids on signal sequence orientation in the endoplasmic reticulum. *J Biol Chem* **275**: 14916-14922.

Sabatini DD, Kreibich G, Morimoto T and Adesnik M (1982) Mechanisms for the incorporation of proteins in membranes and organelles. *J Cell Biol* **92**: 1-22.

Sakaguchi M, Hachiya N, Mihara K and Omura T (1992a) Mitochondrial porin can be translocated across both endoplasmic reticulum and mitochondrial membranes. *J Biochem* **112**: 243-248.

Sakaguchi M, Mihara K and Sato R (1987a) A short amino-terminal segment of microsomal cytochrome P-450 functions both as an insertion signal and as a stop-transfer sequence. *EMBO J* **6**: 2425-2431.

Sakaguchi M, Mihara K and Sato R (1987b) A short amino-terminal segment of microsomal cytochrome P-450 functions both as an insertion signal and as a stop-transfer sequence. *EMBO J* **6**: 2425-2531.

MOL#90431

Sakaguchi M, Tomiyoshi R, Kuroiwa T, Mihara K and Omura T (1992b) Functions of signal and signal-anchor sequences are determined by the balance between the hydrophobic segment and the N-terminal charge. *Proc Natl Acad Sci USA* **89**: 16-19.

Saparov SM, Erlandson K, Cannon K, Schaletzky J, Schulman S, Rapoport TA and Pohl P (2007) Determining the conductance of the SecY protein translocation channel for small molecules. *Mol Cell* **26**: 501-509.

Shimozawa O, Sakaguchi M, Ogawa H, Harada N, Mihara K and Omura T (1993) Core glycosylation of cytochrome P-450(arom). Evidence for localization of N terminus of microsomal cytochrome P-450 in the lumen. *J Biol Chem* **268**: 21399-21402.

Silva MC, Rowlands MG, Dowsett M, Gusterson B, McKinna JA, Fryatt I and Coombes RC (1989) Intratumoral aromatase as a prognostic factor in human breast carcinoma. *Cancer Res* **49**: 2588-2591.

Spiess M and Lodish HF (1986) An internal signal sequence: the asialoglycoprotein receptor membrane anchor. *Cell* **44**: 177-185.

Stern JB and Jackson RC (1985) Peptide products of the cleavage of bovine preprolactin by signal peptidase. *Arch Biochem Biophys* **237**: 244-252.

MOL#90431

Szczesna-Skorupa E, Browne N, Mead D and Kemper B (1988) Positive charges at the NH₂ terminus convert the membrane-anchor signal peptide of cytochrome P-450 to a secretory signal peptide. *Proc Natl Acad Sci USA* **85**: 738-742.

Tam PC, Maillard AP, Chan KK and Duong F (2005) Investigating the SecY plug movement at the SecYEG translocation channel. *EMBO J* **24**: 3380-3388.

Thijssen JH and Blankenstein MA (1989) Endogenous oestrogens and androgens in normal and malignant endometrial and mammary tissues. *Eur J Cancer Clin Oncol* **25**: 1953-1959.

von Heijne G (1986) The distribution of positively charged residues in bacterial inner membrane proteins correlates with the transmembrane topology. *EMBO J* **5**: 3021-3027.

Wahlberg JM and Spiess M (1997) Multiple determinants direct the orientation of signal-anchor proteins: The topogenic role of the hydrophobic signal domain. *J Cell Biol* **137**: 555-562.

Walter P and Johnson AE (1994) Signal sequence recognition and protein targeting to the endoplasmic reticulum membrane. *Annu Rev Cell Biol* **10**: 87-119.

Zerial M, Melancon P, Schneider C and Garoff H (1986) The transmembrane segment of the human transferrin receptor functions as a signal peptide. *EMBO J* **5**: 1543-1550.

MOL#90431

FOOTNOTES:

This work was supported by National Institutes of Health [HD057876] (to HSB) and Anderson Cancer Institute [ACI570107] (to HSB).

MOL#90431

FIGURE LEGENDS

Figure 1. *Topology of glycosylated aromatase*

A) Schematic representation of the steroid hormone synthesis pathway and the role of aromatase. B) Cell-free synthesis (CFS) of [³⁵S]methionine-labeled aromatase with and without MM and treatment with endo H. C) Aromatase CFS, with and without MM, treated with PK and PK plus Triton-X100. D) Membrane integration assay where aromatase CFS (with and without MM) was treated with Na₂CO₃ and supernatant (S) was separated from the membrane fraction (P). E) Top panel shows construction of N-terminal and F)-G) internal deletion mutants of aromatase. Bottom panel shows CFS with MM of these mutants. Δ represents deleted amino acids. Red double lines (//) shows that same number of amino acids were present in full-length (Ar) and all the mutant aromatase proteins. Downwards arrow-head (▼) shows Asn-12 in cartoons and glycosylated aromatase in gels. H) Effect of point mutations at 12th (asparagine, N to threonine, T) and 14th (threonine, T to alanine, A) amino acid residues on glycosylation. I) Cartoon showing the topology of glycosylated aromatase in the ER. Yellow bar depicts endoplasmic reticulum membrane and green vertical bar represents SA-I of aromatase. Four five-point star represents glycosylated Asn-12 due to its luminal localization and red cross (X) represents Asn-180 which is non-glycosylated as it is in the cytosol.

Figure 2. *Effect of aromatase SA-I on passenger protein translocation.*

A) Cartoon shows fusion proteins of aromatase (black bar) and pPL (white bar). Signal sequence of pPL, except the four residues preceding the signal peptidase cleavage site, was replaced with increasing lengths of aromatase N-terminus (first 12, 20, 30, 40 and 50 residues). Downwards arrow-head (▼) shows Asn-12 in aromatase and downwards arrow (↓) is signal peptidase

MOL#90431

cleavage site in pPL. B) CFS with and without MM of fusion proteins in presence and absence of PK. C) CFS with and without MM of aromatase and pPL fusions in presence and absence of Endo H.

Figure 3. *Effect of aromatase signal anchor on passenger protein translocation.*

A) Top panel shows the construction of fusion protein of aromatase first 40 residues (black bar) with full-length DHFR (white bar). Bottom panel shows CFS of fusion protein with and without MM, treated with Endo H. B) 1-40Ar+1-187DHFR CFS with and without MM in presence and absence of MTX. C) Top panel shows fusion protein of aromatase first 40 residues (black bar) with full-length SCC (white bar). Bottom panel shows CFS with and without MM, treated with Endo H. Downwards arrow-head (▼) represents Asn-12 in cartoons and glycosylated proteins in gels. Rightwards arrow (→) shows the precursor (p) form of the fusion protein.

Figure 4. *Effect of internal deletions in signal anchor on aromatase glycosylation.*

A) - D) Top panels show the construction of the deletion mutant proteins of aromatase. (v) represents deleted region in the mutants, (▼) is Asn-12 in aromatase and (//) shows that same number of amino acids were present in full-length (Ar) and all the mutant proteins. Bottom panels show the translation of mutants in presence of MM. Downwards arrow-head (▼) shows glycosylated aromatase.

Figure 5. *Effect of deletions in signal anchor on aromatase glycosylation.*

A) Top panel shows the construction of deletional mutant (NΔ36-40) of aromatase. (v) represents deleted region in the mutant, (▼) is Asn-12 and (//) shows that same number of amino

MOL#90431

acids were present in full-length (Ar) and mutant aromatase protein. Bottom panel show the translation of full-length aromatase (Ar) and NΔ36-40 in presence and absence of MM. Downwards arrow-head (▼) shows glycosylated aromatase. B) Membrane integration assay of NΔ36-40, where CFS (with and without MM) was extracted with Na₂CO₃ and supernatant (S) was separated from the membrane fraction (P). C) Top panel shows effect of point mutations in the region 36-40 on glycosylation of aromatase. L-Leucine, V-Valine, W-Tryptophan, F-Phenylalanine, N-Asparagine, Q-Glutamine. Downwards arrow-head (▼) shows glycosylated aromatase. Bottom panel shows densitometric analysis of glycosylated protein bands in various mutants. D) Left panel shows translation of aromatase, NΔ36-40 and globin in presence and absence of SRP. Right panel shows the densitometric analysis intensity of protein bands in presence and absence of SRP. E) Model presenting possible mechanism of insertion of aromatase in the ER membrane to attain a N_{exo}/C_{cyt} topology. Once the aromatase signal anchor (green bar) is synthesized, it interacts with the translocon. The signal anchor opens the lateral channel toward the lipid bilayer. Next, the protein is integrated in the membrane with N-terminal in the lumen and C-terminal in the cytosol. Red circle (O) shows Asn-12, red four-point star shows glycosylated Asn and red cross (X) shows non-glycosylated Asn site.

Figure 6. SA-I did not block signal sequence-mediated translocation.

A) Construction of fusion protein of aromatase SA-I (first 40 and 50 residues, black bar) with full-length pPL (white bar). Similarly, SA-I of CYP11C2 (black bar) was fused with full-length pPL (white bar). Downwards arrow-head (▼) shows Asn-12 in aromatase and downwards arrow (↓) is the signal sequence cleavage site in pPL. CFS with and without MM of full-length pPL (B) and fusion proteins (C, D and E) in presence and absence of PK. Upward arrow (↑) shows the

MOL#90431

processed soluble secretory protein. F) Membrane integration assay of 1-40Ar+1-229pPL, where CFS (with and without MM) was extracted with Na_2CO_3 and supernatant (S) was separated from the membrane fraction (P).

Figure 7. *SA-I did not block signal sequence-mediated translocation.*

A) Construction of mutant proteins from 1-40Ar+1-229pPL. Three positive charges (at positions 4th, 9th and 12th) in the signal sequence of pPL was subsequently mutated as shown and named accordingly. Downwards arrow-head (▼) represents Asn-12 in aromatase and vertical double arrow-head (⇕) shows signal sequence cleavage site in pPL. Black plus (+) sign shows positive amino acids and red negative sign (-) showed negative amino acids in pPL. D, K and R represent Aspartic acid, Lysine and Arginine respectively. B) Translation of 1-40Ar+1-229pPL and its mutants in presence and absence of MM. Upward arrow (↑) shows the processed soluble secretory protein. C) A model of the mechanism of translocation when SA-I is followed immediately by a full-length secretory protein. Cartoon shows nascent chain being synthesized on cytosolic ribosome. As the signal sequence (cyan collate) follows the SA-I (green bar), it destabilizes the closed state of the translocon due to repulsion between the positive charges of signal sequence and the plug of translocon. It leads to premature opening of the pore towards the luminal exit, potentially allowing the translocation of the protein in the ER lumen. This premature opening halts the opening of lateral exit; and thus the SA-I could not get membrane integrated and subsequently did not block the translocation of the passenger protein. In this way, the pPL signal sequence directed the translocation of both flanking protein domains, and once inside the lumen, signal peptidase (black scissors) cleaved the signal sequence generating a soluble protein. D) Top panel shows construction of fusion protein of aromatase (first 50 and 200

MOL#90431

residues, black bar) with full-length pPL (white bar). Asn-12 in aromatase [downwards arrow-head (▼)] and signal sequence cleavage site in pPL [downwards arrow (↓)] is represented schematically. Bottom panel shows translation of fusion proteins in presence and absence of MM. Glycosylated protein is shown by downward arrow-head (▼) and upward arrow (↑) shows the processed soluble secretory protein. E) A model of the mechanism of translocation when SA-I is separated by a distance from a full-length secretory protein. Once the aromatase signal anchor (green bar) is synthesized, it interacts with the translocon. As signal sequence (cyan collate) is still not completely translated, SA-I gets enough time to open the lateral channel of translocon and undergoes membrane-integration. Therefore, the protein now has a $N_{\text{exo}}/C_{\text{cyto}}$ topology, with its N-terminus glycosylated and following signal sequence resides in the cytosol. Red circle (O) shows Asn-12 and red four-point star shows glycosylated Asn.

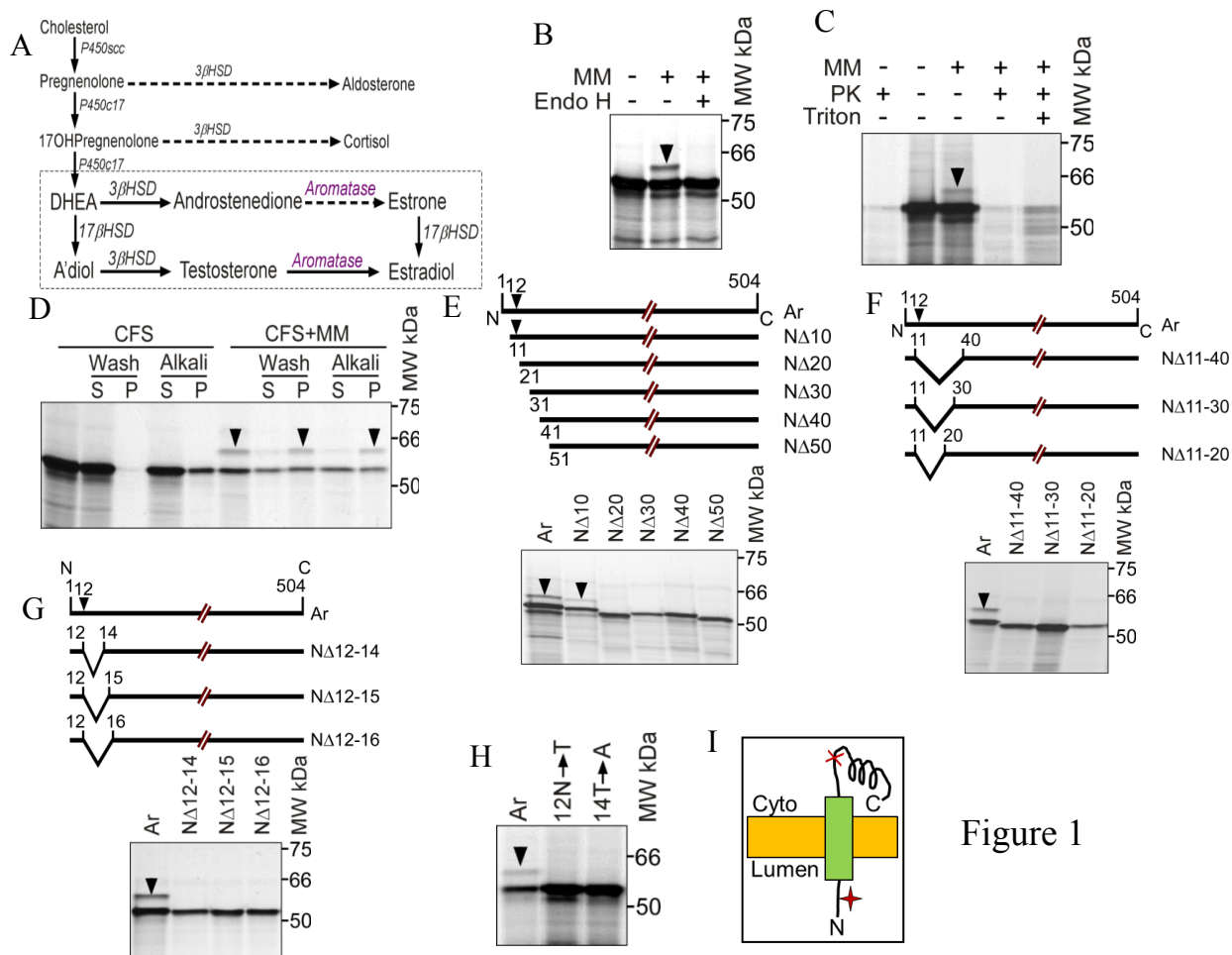


Figure 1

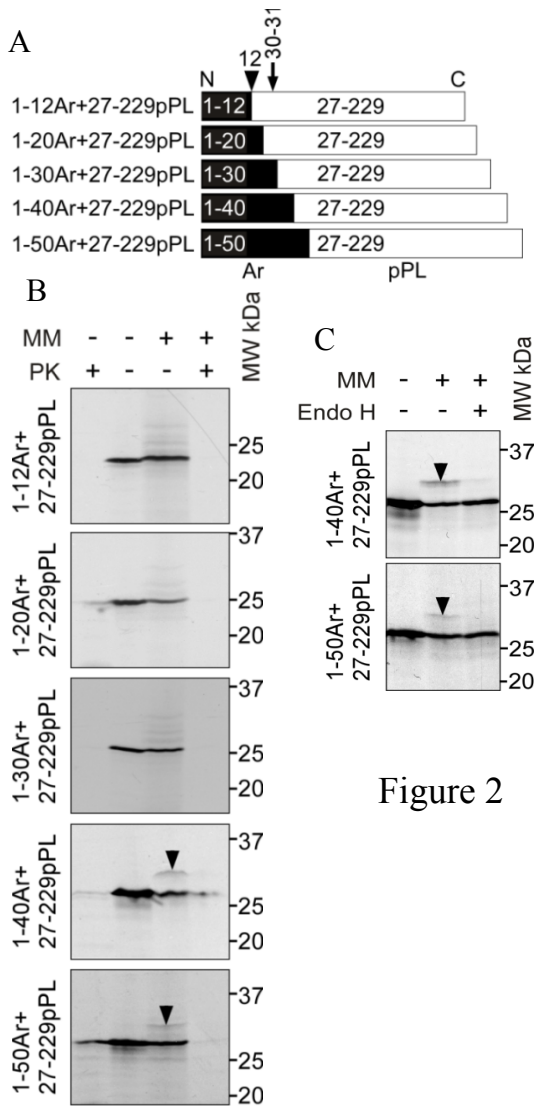


Figure 2

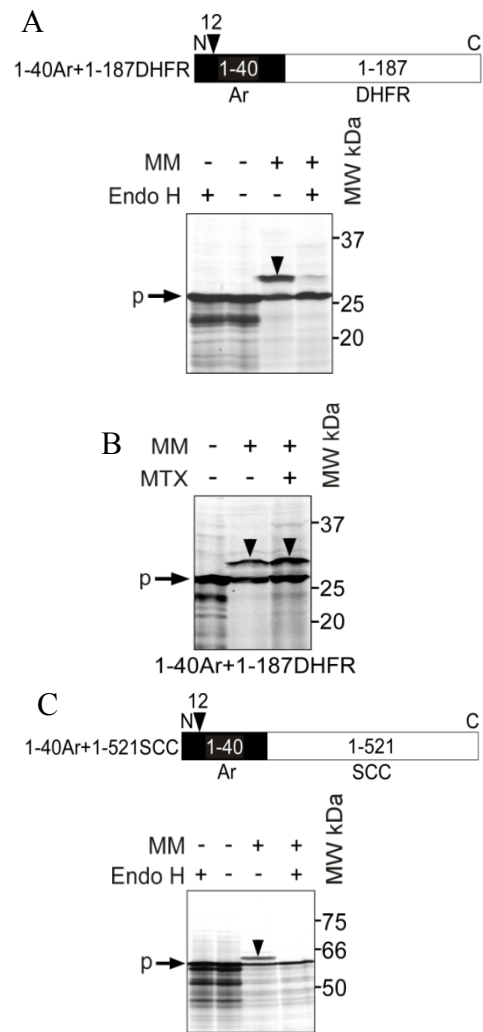


Figure 3

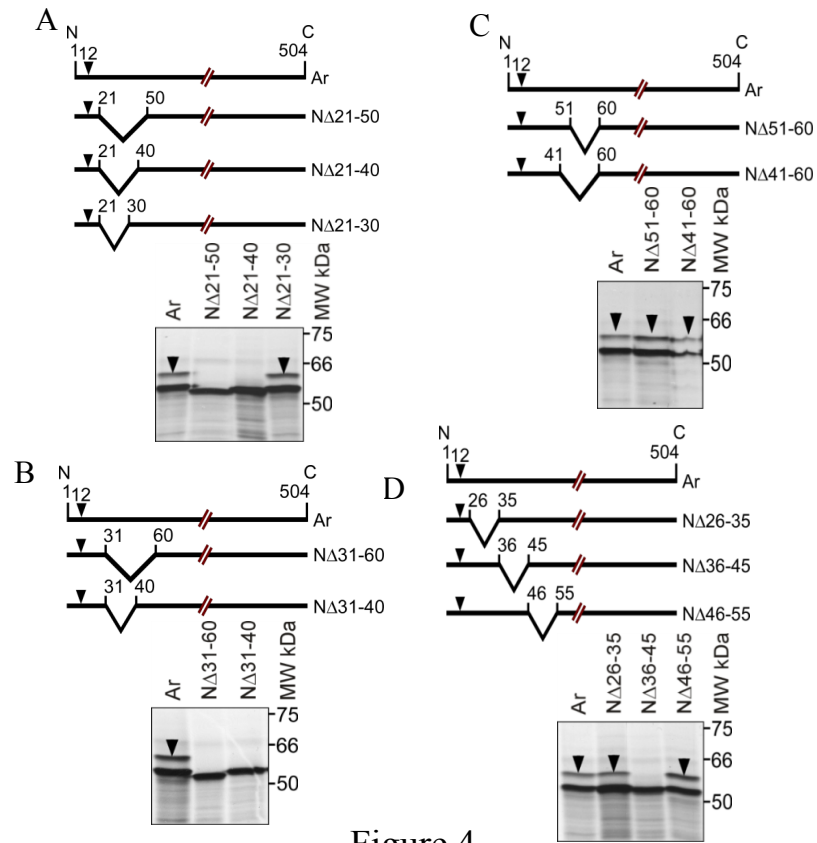


Figure 4

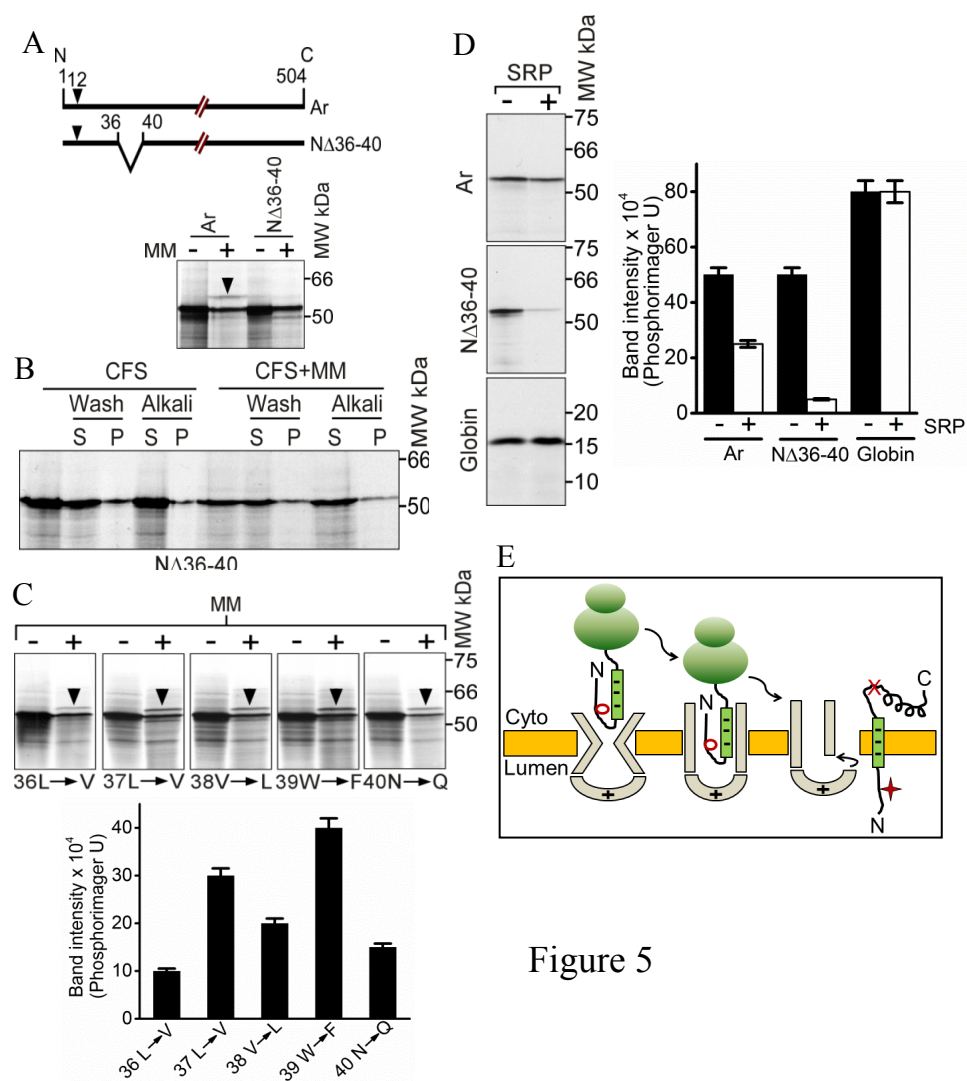


Figure 5

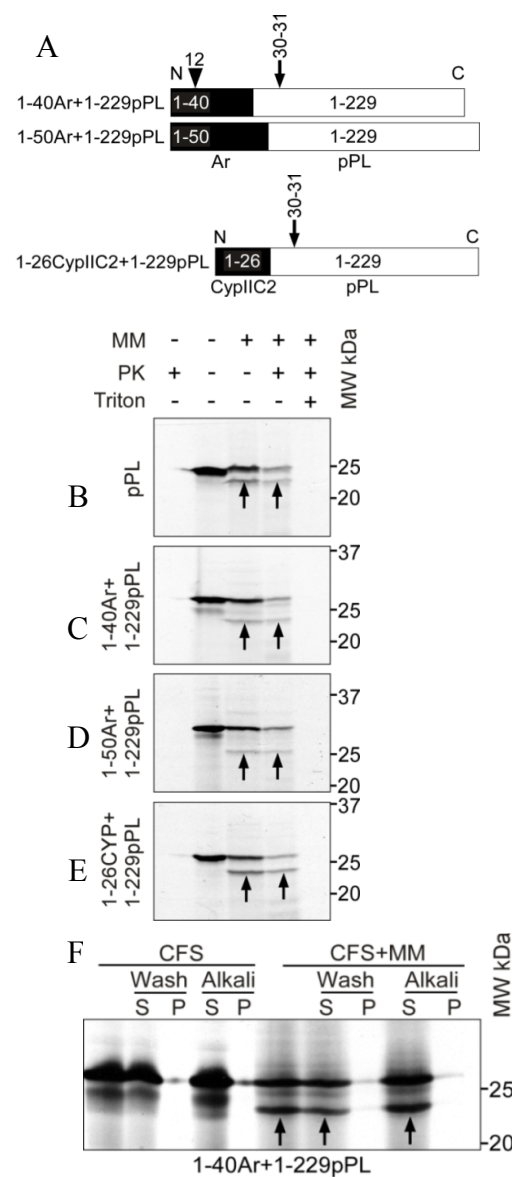


Figure 6

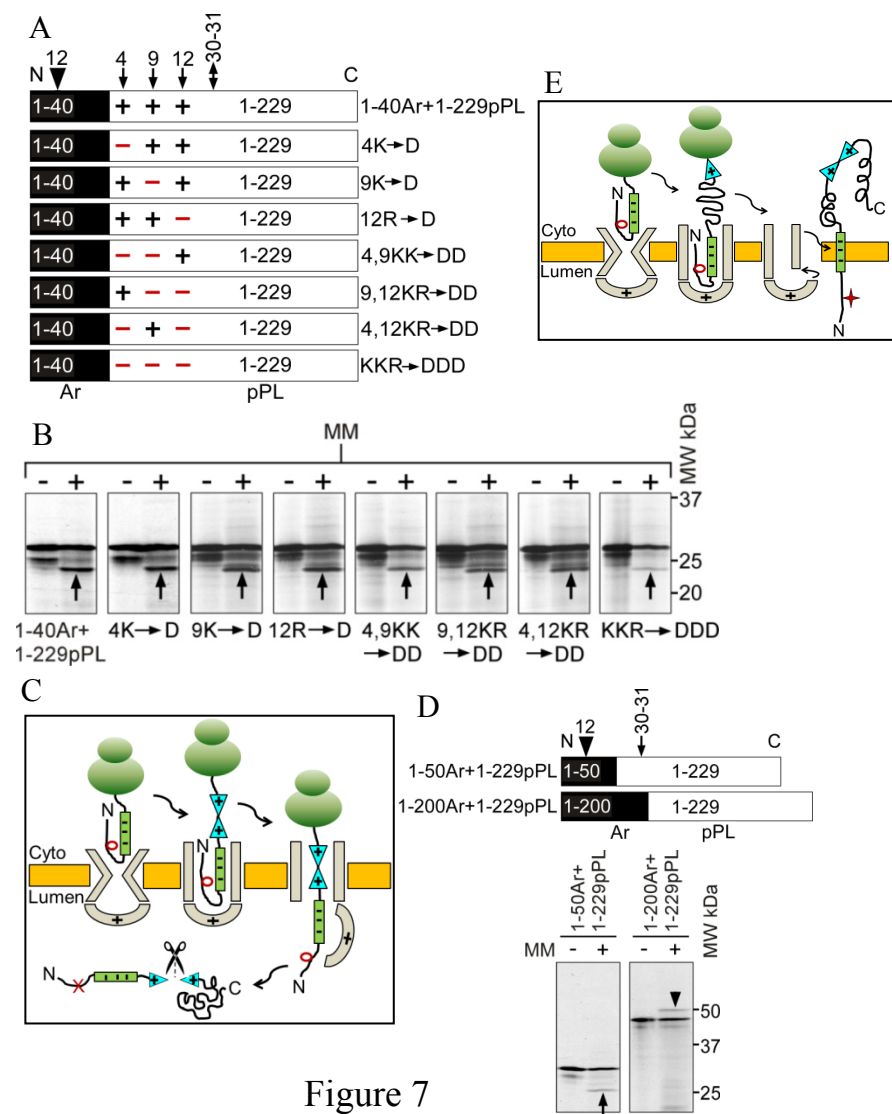


Figure 7